CAPPA: Continuous-Time Accelerated Proximal Point Algorithm for Sparse Recovery

Kunal Garg, *Graduate Student Member, IEEE*, and Mayank Baranwal

***Abstract*—This letter develops a novel Continuous-Time Accelerated Proximal Point Algorithm (CAPPA) for ℓ_1-minimization problems with provable fixed-time convergence guarantees. The problem of ℓ_1-minimization appears in several contexts such as Sparse Recovery (SR) in Compressed Sensing (CS) theory and sparse linear and logistic regressions in machine learning. Most existing algorithms for solving ℓ_1-minimization problems are discrete-time and require exhaustive computer-guided iterations. CAPPA alleviates this problem on two fronts: (a) it encompasses a continuous-time algorithm that can be implemented using analog circuits; (b) it outperforms Locally Competitive Algorithm (LCA) and finite-time LCA (recently developed continuous-time dynamical systems for solving SR problems) by exhibiting provable fixed-time convergence to optimal solution. Consequently, CAPPA is better suited for fast and efficient handling of SR problems.**

***Index Terms*—Compressed sensing, Lyapunov methods, optimization methods, signal reconstruction.**

I. Introduction

Sparse Recovery (SR) or reconstruction of sparse signals from highly-undersampled linear measurements is fundamental to the theory of Compressed Sensing (CS) [1]. Unlike traditional sampling methods, coded measurements in CS require fewer resources in terms of computational time and storage by leveraging simultaneous acquisition and compression of a signal. As a result, SR has applications in several domains, including signal processing [1], [2], medical imaging [3], and machine learning [4]. The major bottleneck in CS is the computational effort required for reconstruction of original signal from its compressed elements. For an observed measurement $\boldsymbol{y} \in \mathbb{R}^M$ corrupted by some noise $\boldsymbol{e} \in \mathbb{R}^M$, SR aims to find a concise representation of a signal $\boldsymbol{x} \in \mathbb{R}^N$ specified as:

$$\boldsymbol{y} = \boldsymbol{\Phi}\boldsymbol{x} + \boldsymbol{e},$$

where $\boldsymbol{\Phi} \in \mathbb{R}^{M\times N}$ is the measurement matrix (with $M \ll N$), and the original signal $\boldsymbol{x}$ is s-sparse, i.e., has no more than s nonzero entries. SR therefore involves an under-determined linear inverse problem, and a unique recovery is guaranteed under certain properties on $\boldsymbol{\Phi}$. The problem of SR can be cast as an equivalent ℓ_1 minimization problem as [5]:

$$\arg\min_{\boldsymbol{x}\in\mathbb{R}^N} \frac{1}{2}\|\boldsymbol{y} - \boldsymbol{\Phi}\boldsymbol{x}\|_2^2 + \lambda\|\boldsymbol{x}\|_1, \tag{P}$$

where $\lambda > 0$ is a balancing parameter. The solution $\boldsymbol{x}^*$ to (P) is referred as the *critical point*. The critical point is unique for an s-sparse signal $\boldsymbol{x}$, provided the measurement matrix $\boldsymbol{\Phi}$ satisfies the Restricted Isometry Property (RIP) with order of $2s$ [6]. While the relaxed optimization problem (P) is convex and computationally tractable, real time SR or implementation on low-power embedded platforms is impractical with most iterative solvers [7]–[10]. While specialized convex solvers are efficient at handling large scale SR problems, they lack strong convergence guarantees about their running time [7], [8]. Subsequently, iterative thresholding schemes were proposed with provable convergence guarantees on number of iterations required to achieve specified accuracy [9]–[11]; however, at the risk of computationally expensive iterations. Recently, several continuous-time algorithms for SR in dynamic environments have been developed [12]–[15]. Besides being implementable on low-power embedded systems, continuous-time algorithms provide novel insights into designing equivalent discrete-time algorithms with accelerated convergence behavior [16], [17].

One such class of continuous-time algorithms, referred to as the Locally Competitive Algorithm (LCA) was proposed in [12]. LCA consists of coupled nonlinear differential equations with a solution trajectory that converges to the minimizer of (P) in steady state. Besides its guaranteed exponential convergence as shown in [18], LCA was also implemented on low-power embedded systems using simple operational amplifiers [19]. LCA was later modified to guarantee finite-time convergence to the critical point in [13]. Finite-time convergence of LCA is related to the notion of finite-time stability of continuous-time dynamical systems introduced in [20]. In contrast to exponential stability, finite-time stability is a concept that guarantees convergence of solutions in a finite amount of time. However, while the convergence time is finite, it depends upon the initial conditions and can grow unbounded as the initial conditions go farther away from the equilibrium point. In contrast, recent work has introduced Fixed-Time Stability (FxTS) [21] where the time of convergence is uniformly bounded for all initial conditions.

In this letter, we present Continuous-Time Accelerated Proximal Point Algorithm (CAPPA) for solving SR problem in a fixed-time. Tools from FxTS theory are leveraged to demonstrate global fixed-time convergence of CAPPA to the critical point. Thus, CAPPA exhibits faster convergence as compared to finite-time LCA in [13]. To this end, the result presented in Lemma 4 translate the RIP condition into an equivalent Lipschitz-gradient and strong convexity condition on the smooth part of the convex objective in (P). Our primary results are presented in Theorem 1,

Manuscript received August 20, 2020; revised September 24, 2020; accepted September 25, 2020. Date of publication September 29, 2020; date of current version October 13, 2020. The associate editor coordinating the review of this manuscript and approving it for publication was Wei Li. *(Corresponding author: Mayank Baranwal.)*

Kunal Garg is with the Department of Aerospace Engineering, University of Michigan, Ann Arbor, MI 48109 USA (e-mail: kgarg@umich.edu).

Mayank Baranwal is with the Tata Consultancy Services Research, Thane, Maharashtra 400607, India (e-mail: baranwal.mayank@tcs.com).

Digital Object Identifier 10.1109/LSP.2020.3027490

where we show that the underlying proximal map is a contraction around the critical point, and Theorem 2, in which the fixed-time convergence of CAPPA is shown.

II. Preliminaries

We use $\mathbb{R}$ to denote the set of real numbers, $\mathcal{C}^1$ to denote the space of continuously differentiable functions, $\|\cdot\|$ to denote the Euclidean norm, unless otherwise specified, and $\langle\cdot\rangle$ to denote the standard inner product on $\mathbb{R}^N$. The $p-$norm is denoted by $\|\cdot\|_p$. While Lemma 2 holds for any proper, closed, lower semi-continuous (lsc) convex functions f, g with $f \in \mathcal{C}^1$, we use $f(\boldsymbol{x})$ and $g(\boldsymbol{x})$ to denote the functions $\frac{1}{2}\|\boldsymbol{y}-\boldsymbol{\Phi x}\|^2$ and $\lambda\|\boldsymbol{x}\|_1$, respectively.

Consider the system:

$$\dot{\boldsymbol{x}}(t) = \boldsymbol{h}(\boldsymbol{x}(t)), \tag{1}$$

where $\boldsymbol{x} \in \mathbb{R}^N$, $\boldsymbol{h}: \mathbb{R}^N \to \mathbb{R}^N$ and $\boldsymbol{h}(\boldsymbol{0}) = \boldsymbol{0}$. Assume that the solution of (1) exists and is unique. As defined in [20], the origin is said to be a finite-time stable equilibrium of (1) if it is Lyapunov stable and *finite-time convergent*, i.e., for all $\boldsymbol{x}(0) \in \mathcal{D}\setminus\{0\}$, where $\mathcal{D}$ is some open neighborhood of the origin, $\lim_{t\to T(\boldsymbol{x}(0))} \boldsymbol{x}(t) = 0$, where $T(\boldsymbol{x}(0)) < \infty$. The authors in [21] presented the following result for FxTS where the time of convergence, i.e., the settling-time function T does not depend on the initial condition $\boldsymbol{x}(0)$.

Lemma 1 ([21]): Suppose there exists a positive definite continuously differentiable function $V: \mathbb{R}^d \to \mathbb{R}$ for system (1) such that $\dot{V}(\boldsymbol{x}(t)) \leq -aV(\boldsymbol{x}(t))^p - bV(\boldsymbol{x}(t))^q$ with $a, b > 0$, $0 < p < 1$ and $q > 1$. Then, the origin of (1) is FxTS, i.e., $\boldsymbol{x}(t) = 0$ for all $t \geq T$, where the settling time T satisfies $T \leq \frac{1}{a(1-p)} + \frac{1}{b(q-1)}$.

We need the following lemmas for proving our main result.

Lemma 2 ([22, Ch.2 Proposition 2.2]): Let $f: \mathbb{R}^N \to \mathbb{R}$, $f \in \mathcal{C}^1$ be a proper, closed convex function, and $g: \mathbb{R}^N \to \mathbb{R}\cup\{\infty\}$ be another proper, closed, lsc convex function (possibly non-smooth). Then, $\boldsymbol{x}^* \in \mathbb{R}^N$ is a minimizer of the sum $f(\cdot) + g(\cdot)$ if and only if

$$\langle \nabla f(\boldsymbol{x}^*), \boldsymbol{x} - \boldsymbol{x}^*\rangle + g(\boldsymbol{x}) - g(\boldsymbol{x}^*) \geq 0, \quad \forall \boldsymbol{x} \in \mathbb{R}^N. \tag{2}$$

Lemma 3 ([23]): For every $c \in (0,1)$, there exists $\epsilon = \frac{\log(c)}{\log(\frac{1-c}{1+c})} > 0$ such that $(\frac{1-c}{1+c})^{1-\alpha} > c, \quad \forall \alpha \in (1-\epsilon, 1)\bigcup(1,\infty)$.

Unique solution of (P) is guaranteed under some assumptions on the matrix $\boldsymbol{\Phi}$. One such assumption is the Restricted Isometry Property (RIP) [6], defined as follows.

Definition 1: Matrix $\boldsymbol{\Phi} \in \mathbb{R}^{M\times N}$ is said to satisfy the order-s RIP for some postive integer s with constant $\delta_s > 0$ if for every s-sparse vector $\boldsymbol{x} \in \mathbb{R}^N$, the following holds true

$$(1-\delta_s)\|\boldsymbol{x}\|_2^2 \leq \|\boldsymbol{\Phi x}\|_2^2 \leq (1+\delta_s)\|\boldsymbol{x}\|_2^2.$$

Using the notion of RIP, we can state the following result, which shows Lipschitz continuity and strong-monotonicity of $\mathbf{F} = \nabla f$, where $f = \frac{1}{2}\|\boldsymbol{y}-\boldsymbol{\Phi x}\|_2^2$ (latter is equivalent to strong-convexity of f).

Lemma 4: Let $\mathbf{F}: \mathbb{R}^N \to \mathbb{R}^N$ be defined as gradient of $\frac{1}{2}\|\boldsymbol{y}-\boldsymbol{\Phi x}\|_2^2$, given as

$$\mathbf{F}(\cdot) := (\boldsymbol{\Phi}^\mathsf{T}\boldsymbol{\Phi})(\cdot) - \boldsymbol{\Phi}^\mathsf{T}\boldsymbol{y}, \tag{3}$$

for any given $\boldsymbol{y} \in \mathbb{R}^M$, where $\boldsymbol{\Phi}$ satisfies order $2s$ RIP with $\delta_{2s} > 0$ for some $s \in \mathbb{Z}_+$. Then

i) $\mathbf{F}$ is Lipschitz continuous on the space of s-sparse vectors in $\mathbb{R}^N$ with modulus $\|\boldsymbol{\Phi}\|_2\sqrt{(1+\delta_{2s})}$;

ii) For any s-sparse $\boldsymbol{x}_1, \boldsymbol{x}_2 \in \mathbb{R}^N$

$$\langle \mathbf{F}(\boldsymbol{x}_1) - \mathbf{F}(\boldsymbol{x}_2), \boldsymbol{x}_1 - \boldsymbol{x}_2\rangle \geq (1-\delta_{2s})\|(\boldsymbol{x}_1 - \boldsymbol{x}_2\|_2^2.$$

Proof.: From the definition of $\mathbf{F}$, it follows that for any s-sparse $\boldsymbol{x}_1, \boldsymbol{x}_2 \in \mathbb{R}^N$,

$$\mathbf{F}(\boldsymbol{x}_1) - \mathbf{F}(\boldsymbol{x}_2) = \boldsymbol{\Phi}^T(\boldsymbol{\Phi}(\boldsymbol{x}_1 - \boldsymbol{x}_2))$$
$$\Rightarrow \quad \|\mathbf{F}(\boldsymbol{x}_1) - \mathbf{F}(\boldsymbol{x}_2)\|_2 \leq \|\boldsymbol{\Phi}\|_2\|\boldsymbol{\Phi}(\boldsymbol{x}_1 - \boldsymbol{x}_2)\|_2, \tag{4}$$

where the last inequality follows from the submultiplicative inequality of matrix-vector product and the fact that 2-norm of a matrix is same as that of its transpose. Since $\boldsymbol{x}_1, \boldsymbol{x}_2$ are s-sparse, $\boldsymbol{x}_1 - \boldsymbol{x}_2$ is at most $2s$-sparse. Thus, from (4) and the right-hand side of the RIP, it follows that

$$\|\mathbf{F}(\boldsymbol{x}_1) - \mathbf{F}(\boldsymbol{x}_2)\|_2 \leq \|\boldsymbol{\Phi}\|_2\sqrt{(1+\delta_{2s})}\|(\boldsymbol{x}_1 - \boldsymbol{x}_2)\|_2,$$

i.e., $\mathbf{F}$ is Lipschitz with modulus $\|\boldsymbol{\Phi}\|_2\sqrt{(1+\delta_{2s})}$.

Again from the definition of the operator $\mathbf{F}$, it follows that

$$\langle \mathbf{F}(\boldsymbol{x}_1) - \mathbf{F}(\boldsymbol{x}_2), \boldsymbol{x}_1 - \boldsymbol{x}_2\rangle = \|\boldsymbol{\Phi}(\boldsymbol{x}_1 - \boldsymbol{x}_2)\|_2^2$$
$$\langle \mathbf{F}(\boldsymbol{x}_1) - \mathbf{F}(\boldsymbol{x}_2), \boldsymbol{x}_1 - \boldsymbol{x}_2\rangle \geq (1-\delta_{2s})\|\boldsymbol{x}_1 - \boldsymbol{x}_2\|_2^2, \tag{5}$$

where the last inequality follows directly from RIP. ■

III. Main Results

We now present the fixed-time stable dynamical system designed for CAPPA to find the solution of (P) using a proximal flow approach. It is shown that the solution of the modified Proximal Dynamical System (PDS) converges to its equilibrium point (which is also the solution of (P)) within a fixed time.

The nominal PDS for the problem (P) is given as

$$\dot{\boldsymbol{x}} = -(\boldsymbol{x} - \text{prox}_{\eta g}(\boldsymbol{x} - \eta\,\mathbf{F}(\boldsymbol{x}))), \tag{6}$$

where $\mathbf{F}$ is defined as in (3). It has been shown that under certain conditions on $\mathbf{F}$, the solution $\boldsymbol{x}^*$ of (6) exponentially converges to the optimal solution of (P) (see, e.g., [24]). Using this, we define a modification of this PDS so that the convergence can be guaranteed within a fixed time. Consider the modified PDS:

$$\dot{\boldsymbol{x}} = -\kappa_1\frac{\boldsymbol{x} - \boldsymbol{z}(\boldsymbol{x})}{\|\boldsymbol{x} - \boldsymbol{z}(\boldsymbol{x})\|_2^{1-\alpha_1}} - \kappa_2\frac{\boldsymbol{x} - \boldsymbol{z}(\boldsymbol{x})}{\|\boldsymbol{x} - \boldsymbol{z}(\boldsymbol{x})\|_2^{1-\alpha_2}},$$
$$\boldsymbol{z}(\boldsymbol{x}) = \text{prox}_{\eta g}(\boldsymbol{x} - \eta\,\mathbf{F}(\boldsymbol{x}))$$
$$= \text{sign}(\boldsymbol{x} - \eta\,\mathbf{F}(\boldsymbol{x}))\cdot\max(|\boldsymbol{x} - \eta\,\mathbf{F}(\boldsymbol{x})| - \eta\lambda, 0) \tag{7}$$

where $\eta > 0$, $\alpha_1 \in (0,1)$, $\alpha_2 > 1$, $\kappa_1, \kappa_2 > 0$ and $g(\boldsymbol{x}) = \lambda\|\boldsymbol{x}\|_1$. Here $\mathbf{F}(\cdot)$ is as defined in (3), and denotes the gradient ∇f of the function $f(\boldsymbol{x}) = \frac{1}{2}\|\boldsymbol{y}-\boldsymbol{\Phi x}\|_2^2$ for a fixed $\boldsymbol{y}$, while the operators $|\cdot|$, $\max$ and $sign$ are applied element-wise. Note that the equilibrium point of (7) and the solution of (P) are the same (see [25, Proposition 12.26]) and the fact that for any equilibrium point $\bar{\boldsymbol{x}}$ of (7), $\bar{\boldsymbol{x}} = z(\bar{\boldsymbol{x}})$. We assume that $\boldsymbol{\Phi}$ satisfies order $2s$ RIP with $\delta_{2s} > 0$.

Next, we prove an intermediate result on the contraction property of proximal flows.

Theorem 1: For every $\eta \in (0, \frac{2(1-\delta_{2s})}{\|\boldsymbol{\Phi}\|_2^2(1+\delta_{2s})})$, there exists $c \in (0,1)$ such that

$$\|\boldsymbol{z}(\boldsymbol{x}) - \boldsymbol{x}^*\|_2 \leq c\|\boldsymbol{x} - \boldsymbol{x}^*\|_2,$$

for all s-sparse $\boldsymbol{x} \in \mathbb{R}^N$, where $\boldsymbol{x}^* \in \mathbb{R}^N$ is a solution of (P), $\boldsymbol{z}(\boldsymbol{x}) := \text{prox}_{\eta g}(\boldsymbol{x} - \eta\, \mathbf{F}(\boldsymbol{x}))$ and $\mathbf{F}$ is as defined in (3).

Proof.: From [25, Proposition 12.26], for any given $\boldsymbol{x} \in \mathbb{R}^N$

$$\langle \boldsymbol{z}(\boldsymbol{x}) - (\boldsymbol{x} - \eta\, \mathbf{F}(\boldsymbol{x}), \boldsymbol{q} - \boldsymbol{z}(\boldsymbol{x})\rangle \geq \eta\,(g(\boldsymbol{z}(\boldsymbol{x})) - g(\boldsymbol{q})) \quad (8)$$

for all $\boldsymbol{q} \in \mathbb{R}^N$. In particular, for $\boldsymbol{q} = \boldsymbol{x}^*$ and after making some re-arrangements, (8) reads:

$$\langle \boldsymbol{z}(\boldsymbol{x}) - \boldsymbol{x}, \boldsymbol{x}^* - \boldsymbol{z}(\boldsymbol{x})\rangle \geq \eta\,(g(\boldsymbol{z}(\boldsymbol{x})) - g(\boldsymbol{x}^*)) + \eta\, \mathbf{F}(\boldsymbol{x})^\intercal\,(\boldsymbol{z}(\boldsymbol{x}) - \boldsymbol{x}^*) \quad (9)$$

Furthermore, from Lemma 2, it follows that

$$\eta\,(g(\boldsymbol{z}(\boldsymbol{x})) - g(\boldsymbol{x}^*)) \geq \eta\, \mathbf{F}(\boldsymbol{x}^*)^\intercal(\boldsymbol{x}^* - \boldsymbol{z}(\boldsymbol{x})). \quad (10)$$

Using (9) and (10), we obtain that

$$\langle \boldsymbol{x} - \boldsymbol{z}(\boldsymbol{x}), \boldsymbol{x}^* - \boldsymbol{z}(\boldsymbol{x})\rangle \leq \eta\, \langle \mathbf{F}(\boldsymbol{x}^*) - \mathbf{F}(\boldsymbol{x}), \boldsymbol{z}(\boldsymbol{x}) - \boldsymbol{x}^*\rangle,$$

which can be rewritten as

$$\langle \boldsymbol{x} - \boldsymbol{z}(\boldsymbol{x}), \boldsymbol{x}^* - \boldsymbol{z}(\boldsymbol{x})\rangle \leq \eta\, \langle \mathbf{F}(\boldsymbol{x}^*) - \mathbf{F}(\boldsymbol{z}(\boldsymbol{x}), \boldsymbol{z}(\boldsymbol{x}) - \boldsymbol{x}^*\rangle + \eta\, \langle \mathbf{F}(\boldsymbol{z}(\boldsymbol{x})) - \mathbf{F}(\boldsymbol{x}), \boldsymbol{z}(\boldsymbol{x}) - \boldsymbol{x}^*\rangle. \quad (11)$$

From Lemma 4, the first term in the right hand side of (11) can be upper bounded as follows:

$$\eta\, \langle \mathbf{F}(\boldsymbol{x}^*) - \mathbf{F}(\boldsymbol{z}(\boldsymbol{x}), \boldsymbol{z}(\boldsymbol{x}) - \boldsymbol{x}^*\rangle \leq -\eta(1 - \delta_{2s})\|\boldsymbol{x}^* - \boldsymbol{z}(\boldsymbol{x})\|^2. \quad (12)$$

Using the Cauchy–Schwarz inequality and again from Lemma 4, the second term in the right hand side of (11) can be upper bounded as follows:

$$\eta\, \langle \mathbf{F}(\boldsymbol{z}(\boldsymbol{x})) - \mathbf{F}(\boldsymbol{x}), \boldsymbol{z}(\boldsymbol{x}) - \boldsymbol{x}^*\rangle \leq \lambda L\|\boldsymbol{x} - \boldsymbol{z}(\boldsymbol{x})\|\|\boldsymbol{x}^* - \boldsymbol{z}(\boldsymbol{x})\|, \quad (13)$$

where $L := \|\boldsymbol{\Phi}\|_2\sqrt{1 + \delta_{2s}}$. Using Cauchy's inequality, the right hand side of (13) can further be upper bounded as follows:

$$\eta L\|\boldsymbol{x} - \boldsymbol{z}(\boldsymbol{x})\|\|\boldsymbol{x}^* - \boldsymbol{z}(\boldsymbol{x})\| \leq \frac{1}{2}\|\boldsymbol{x} - \boldsymbol{z}(\boldsymbol{x})\|^2 + \frac{(\eta L)^2}{2}\|\boldsymbol{x}^* - \boldsymbol{z}(\boldsymbol{x})\|^2$$

and so, (13) results into:

$$\eta\, \langle \mathbf{F}(\boldsymbol{z}(\boldsymbol{x})) - \mathbf{F}(\boldsymbol{x}), \boldsymbol{z}(\boldsymbol{x}) - \boldsymbol{x}^*\rangle \leq \frac{(\eta L)^2}{2}\|\boldsymbol{x}^* - \boldsymbol{z}(\boldsymbol{x})\|^2 + \frac{1}{2}\|\boldsymbol{x} - \boldsymbol{z}(\boldsymbol{x})\|^2. \quad (14)$$

Using (12) and (14), the right hand side of (11) can be upper bounded as follows:

$$\langle \boldsymbol{x} - \boldsymbol{z}(\boldsymbol{x}), \boldsymbol{x}^* - \boldsymbol{z}(\boldsymbol{x})\rangle \leq -\eta\, \mu\, \|\boldsymbol{x}^* - \boldsymbol{z}(\boldsymbol{x})\|^2 + \frac{1}{2}\|\boldsymbol{x} - \boldsymbol{z}(\boldsymbol{x})\|^2 + \frac{\eta^2 L^2}{2}\|\boldsymbol{x}^* - \boldsymbol{z}(\boldsymbol{x})\|^2, \quad (15)$$

where $\mu := (1 - \delta_{2s})$. Furthermore, the left hand side of (15) can be rewritten as:

$$\langle \boldsymbol{x} - \boldsymbol{z}(\boldsymbol{x}), \boldsymbol{x}^* - \boldsymbol{z}(\boldsymbol{x})\rangle = \frac{1}{2}\|\boldsymbol{x} - \boldsymbol{z}(\boldsymbol{x})\|^2 + \frac{1}{2}\|\boldsymbol{x}^* - \boldsymbol{z}(\boldsymbol{x})\|^2 - \frac{1}{2}\|\boldsymbol{x} - \boldsymbol{x}^*\|^2. \quad (16)$$

Using (15) and (16), we obtain that

$$\|\boldsymbol{x} - \boldsymbol{z}(\boldsymbol{x})\|^2 + \|\boldsymbol{x}^* - \boldsymbol{z}(\boldsymbol{x})\|^2 - \|\boldsymbol{x} - \boldsymbol{x}^*\|^2 \leq \|\boldsymbol{x} - \boldsymbol{z}(\boldsymbol{x})\|^2 + \eta^2 L^2\|\boldsymbol{x}^* - \boldsymbol{z}(\boldsymbol{x})\|^2 - 2\eta\mu\|\boldsymbol{x}^* - \boldsymbol{z}(\boldsymbol{x})\|^2,$$

which simplifies to

$$\|\boldsymbol{z}(\boldsymbol{x}) - \boldsymbol{x}^*\|^2 \leq \bar{c}\|\boldsymbol{x} - \boldsymbol{x}^*\|^2, \quad (17)$$

with $\bar{c} = 1/(1 + 2\eta\mu - \eta^2 L^2)$. Note that $\bar{c} \in (0, 1)$, since by assumption, $\eta \in (0, \frac{2\mu}{L^2})$ and so, (17) can be rewritten as

$$\|\boldsymbol{z}(\boldsymbol{x}) - \boldsymbol{x}^*\| \leq c\|\boldsymbol{x} - \boldsymbol{x}^*\|,$$

where $c := \sqrt{\bar{c}} \in (0, 1)$. ∎

We are now ready to present our main result.

Theorem 2: For every $\eta \in (0, \frac{2(1-\delta_{2s})}{\|\boldsymbol{\Phi}\|_2^2(1+\delta_{2s})})$, there exists $\varepsilon > 0$ such that the solution $\boldsymbol{x}^* \in \mathbb{R}^N$ of (P) is a globally FxTS equilibrium point of (7) for any $\alpha_1 \in (1 - \varepsilon, 1) \cap (0, 1)$ and $\alpha_2 > 1$.

Proof.: Consider the candidate Lyapunov function $V : \mathbb{R}^N \to \mathbb{R}$ defined as follows:

$$V(\boldsymbol{x}) := \frac{1}{2}\|\boldsymbol{x} - \boldsymbol{x}^*\|^2,$$

where $\boldsymbol{x}^*$ is the unique equilibrium point of the proposed (7). It is clear that V is positive definite and radially unbounded. Note that $\boldsymbol{x}^*$ is also the unique minimizer of the sum $f(\cdot) + g(\cdot)$. The time-derivative of V along the solution of (7), starting from any s-sparse $\boldsymbol{x}(0) \in \mathbb{R}^N \setminus \{\boldsymbol{x}^*\}$, reads:

$$\begin{aligned}\dot{V} &= -\kappa_1\frac{\langle \boldsymbol{x} - \boldsymbol{x}^*, \boldsymbol{x} - \boldsymbol{z}(\boldsymbol{x})\rangle}{\|\boldsymbol{x} - \boldsymbol{z}(\boldsymbol{x})\|^{1-\alpha_1}} - \kappa_2\frac{\langle \boldsymbol{x} - \boldsymbol{x}^*, \boldsymbol{x} - \boldsymbol{z}(\boldsymbol{x})\rangle}{\|\boldsymbol{x} - \boldsymbol{z}(\boldsymbol{x})\|^{1-\alpha_2}} \\ &= -\kappa_1\frac{\langle \boldsymbol{x} - \boldsymbol{x}^*, \boldsymbol{x} - \boldsymbol{x}^*\rangle}{\|\boldsymbol{x} - \boldsymbol{z}(\boldsymbol{x})\|^{1-\alpha_1}} - \kappa_2\frac{\langle \boldsymbol{x} - \boldsymbol{x}^*, \boldsymbol{x} - \boldsymbol{x}^*\rangle}{\|\boldsymbol{x} - \boldsymbol{z}(\boldsymbol{x})\|^{1-\alpha_2}} \\ &\quad - \kappa_1\frac{\langle \boldsymbol{x}^* - \boldsymbol{z}(\boldsymbol{x}), \boldsymbol{x} - \boldsymbol{x}^*\rangle}{\|\boldsymbol{x} - \boldsymbol{z}(\boldsymbol{x})\|^{1-\alpha_1}} - \kappa_2\frac{\langle \boldsymbol{x}^* - \boldsymbol{z}(\boldsymbol{x}), \boldsymbol{x} - \boldsymbol{x}^*\rangle}{\|\boldsymbol{x} - \boldsymbol{z}(\boldsymbol{x})\|^{1-\alpha_2}}.\end{aligned} \quad (18)$$

Using the Cauchy–Schwarz inequality, (18) translates to:

$$\begin{aligned}\dot{V} &\leq -\left(\kappa_1\frac{\|\boldsymbol{x} - \boldsymbol{x}^*\|^2}{\|\boldsymbol{x} - \boldsymbol{z}(\boldsymbol{x})\|^{1-\alpha_1}} + \kappa_2\frac{\|\boldsymbol{x} - \boldsymbol{x}^*\|^2}{\|\boldsymbol{x} - \boldsymbol{z}(\boldsymbol{x})\|^{1-\alpha_2}}\right) \\ &\quad + \left(\kappa_1\frac{\|\boldsymbol{x} - \boldsymbol{x}^*\|\|\boldsymbol{x}^* - \boldsymbol{z}(\boldsymbol{x})\|}{\|\boldsymbol{x} - \boldsymbol{z}(\boldsymbol{x})\|^{1-\alpha_1}} + \kappa_2\frac{\|\boldsymbol{x} - \boldsymbol{x}^*\|\|\boldsymbol{x}^* - \boldsymbol{z}(\boldsymbol{x})\|}{\|\boldsymbol{x} - \boldsymbol{z}(\boldsymbol{x})\|^{1-\alpha_2}}\right).\end{aligned} \quad (19)$$

From Theorem 1, for $\eta \in (0, 2(1 - \delta_{2s})/(\|\boldsymbol{\Phi}\|^2(1 + \delta_{2s})))$,

$$\|\boldsymbol{x} - \boldsymbol{z}(\boldsymbol{x})\| \leq \|\boldsymbol{x} - \boldsymbol{x}^*\| + \|\boldsymbol{x}^* - \boldsymbol{z}(\boldsymbol{x})\| \leq (1 + c)\|\boldsymbol{x} - \boldsymbol{x}^*\|, \quad (20)$$

holds for all s-sparse $\boldsymbol{x} \in \mathbb{R}^N$, where $c \in (0, 1)$. Similarly,

$$\|\boldsymbol{x} - \boldsymbol{z}(\boldsymbol{x})\| \geq (1 - c)\|\boldsymbol{x} - \boldsymbol{x}^*\|, \quad (21)$$

also holds for all $\boldsymbol{x} \in \mathbb{R}^N$. Using (20), (21) and Theorem 1, the right hand side of (19) can further be upper bounded as

$$\begin{aligned}\dot{V} &\leq -\left(\frac{\kappa_1\|\boldsymbol{x} - \boldsymbol{x}^*\|^2}{((1 + c)\|\boldsymbol{x} - \boldsymbol{x}^*\|)^{1-\alpha_1}} + \frac{\kappa_2\|\boldsymbol{x} - \boldsymbol{x}^*\|^2}{((1 + c)\|\boldsymbol{x} - \boldsymbol{x}^*\|)^{1-\alpha_2}}\right) \\ &\quad + \left(\frac{c\kappa_1\|\boldsymbol{x} - \boldsymbol{x}^*\|^2}{((1 - c)\|\boldsymbol{x} - \boldsymbol{x}^*\|)^{1-\alpha_1}} + \frac{c\kappa_2\|\boldsymbol{x} - \boldsymbol{x}^*\|^2}{((1 - c)\|\boldsymbol{x} - \boldsymbol{x}^*\|)^{1-\alpha_2}}\right) \\ &= -s_1\|\boldsymbol{x} - \boldsymbol{x}^*\|^{1+\alpha_1} - s_2\|\boldsymbol{x} - \boldsymbol{x}^*\|^{1+\alpha_2},\end{aligned} \quad (22)$$

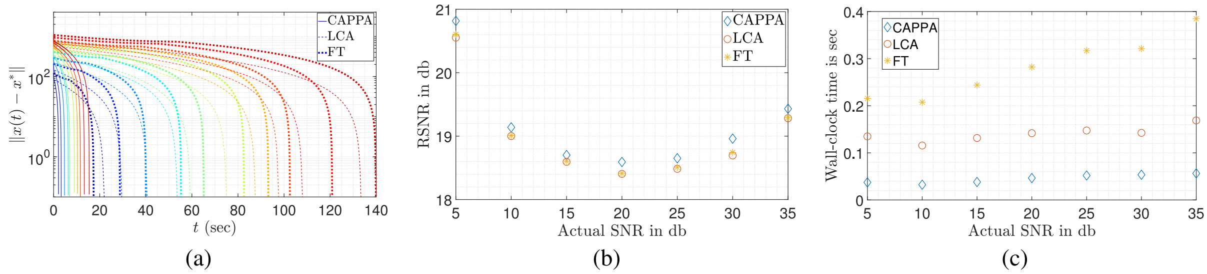

Fig. 1. Comparison of the proposed CAPPA, LCA and and the finite-time LCA for $N = 400, M = 200, s = 20$ (a) Error $\|\boldsymbol{x}(t) - \boldsymbol{x}_{fmin}\|$ with time for various initial conditions. (b) Reconstruction SNR for various values of ASNR. (c) Wall-clock time for various ASNR.

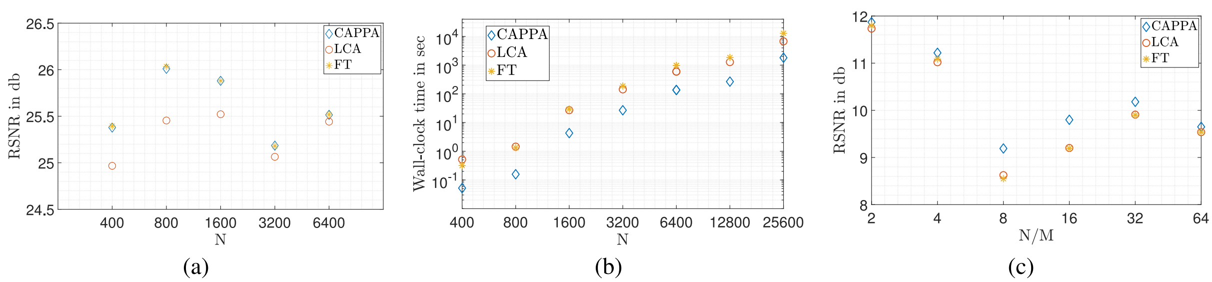

Fig. 2. Comparative analysis of the proposed CAPPA, LCA and and the finite-time LCA for varying sizes of sparse vector and measurement matrix (a) RSNR for various values of N. (b) Wall-clock time for various values of N. (c) RSNR for various values of the ratio $\frac{N}{M}$.

with s_1, s_2 chosen accordingly. From Lemma 3, it follows that there exists $\epsilon(c) = \frac{\log(c)}{\log(\frac{1-c}{1+c})} > 0$ such that (22) results into:

$$\dot{V} \leq -\left(a_1(\alpha_1)V^{\gamma_1(\alpha_1)} + a_2(\alpha_2)V^{\gamma_2(\alpha_2)}\right),$$

with $a_1(\alpha_1) := 2^{\gamma_1(\alpha_1)}q_1(\alpha_1) > 0$ for any $\alpha_1 \in (1 - \epsilon(c), 1) \cap (0, 1)$, where $\gamma_1(\alpha_1) := \frac{1+\alpha_1}{2} \in (0.5, 1)$ and $a_2(\alpha_2) := 2^{\gamma_2(\alpha_2)}q_2(\alpha_2) > 0$ for any $\alpha_2 > 1$, where $\gamma_2(\alpha_2) := \frac{1+\alpha_2}{2} > 1$. The proof follows Lemma 1. ∎

IV. Numerical Experiment

We now present numerical experiments performed using MATLAB R2018a on an Intel Xeon E3-1245 desktop (3.4 GHz). Euler discretization with constant step-size $dt = 10^{-4}$ is used. The matrix $\boldsymbol{\Phi} \in \mathbb{R}^{M \times N}$ is drawn from a normal Gaussian distribution (and normalized to make every column with unit norm), and the noise $\boldsymbol{e}$ is chosen as additive white Gaussian noise of varying signal-to-noise ratio (SNR). The parameters for CAPPA are chosen as $a_1 = 0.1, a_2 = 1.1, k_1 = k_2 = 50, \lambda = 0.05, \eta = 0.4$. We compare the performance of the proposed scheme with the nominal LCA scheme as well as the finite-time variant of the LCA scheme in [13]. The parameters for LCA and finite-time LCA (denoted as FT in the figures), are same as in [13]. We use the MATLAB function `fmicon` to compute an estimate of $\boldsymbol{x}^*$ (denoted as $\boldsymbol{x}_{fmin}$) for the sake of comparison.

Fig. 1a shows the evolution of the error vector $\|\boldsymbol{x}(t) - \boldsymbol{x}_{fmin}\|$ with time for various initial conditions for the proposed CAPPA, the LCA and the FT methods for $N = 400, M = 200, s = 20$ [13]. It is clear that CAPPA converges to the optimal solution within a fixed time irrespective of the initial conditions, and has a faster convergence as compared to LCA or FT.

CAPPA is also robust to measurement noise due to inherent robustness properties of FxTS systems. This is captured in Fig. 1b by plotting reconstructed signal-to-noise ratio (RSNR), defined as $\text{RSNR}(\boldsymbol{x}) = -10\log_{10}(\frac{\|\boldsymbol{\Phi x}^* - \boldsymbol{\Phi x}\|}{\|\boldsymbol{\Phi x}^*\|})$, averaged over 100 trials, against varying levels of actual SNR (ASNR), defined as ASNR$= -10\log_{10}(\frac{\|\boldsymbol{e}\|}{\|\boldsymbol{\Phi x}^*\|})$. The corresponding run-times (in wall-clock time) for the three algorithms are shown in Fig. 1c. It can be observed that CAPPA is not only an order of magnitude faster than the LCA and FT methods, the quality of reconstruction of the signal is also better.

We further evaluate CAPPA for large N. Figs. 2a and 2b depict the RSNRs and wall-clock times, respectively, for various values of N with fixed ratios $\frac{N}{M} = 2$ and $\frac{N}{s}$. CAPPA scales efficiently as N is increased in comparison to the LCA and the FT methods, while still ensuring superior RSNR as compared to the other two methods. The final set of experiments explores performance of CAPPA for different ratios of $\frac{N}{M}$ for fixed values of ASNR$=$ 20dB, $N = 1024$, and $\frac{M}{s} = 10$, while M is varied. These numerical studies show that CAPPA is capable of handling large values of N, as well as large ratios of $\frac{N}{M}$ while being able to reconstruct the signal with better SNR in a reasonable computational time.

V. Conclusion and Future Work

In this letter, we present CAPPA algorithm for addressing the problem of Sparse Recovery under RIP condition on the measurement matrix. The proposed algorithm exhibits fixed-time convergence to the unique critical point of (P). Compared to LCA (or its finite-time modification), CAPPA is shown to achieve faster convergence in numerical experiment, both in number of iterations, as well as in wall-clock time. It is shown in [26] that discrete-time implementation of LCA resembles the soft iterative thresholding methods for SR, which encourages us to explore equivalent discrete-time versions of CAPPA.

REFERENCES

[1] E. J. Candès and M. B. Wakin, "An introduction to compressive sampling," *IEEE Signal Process. Mag.*, vol. 25, no. 2, pp. 21–30, Mar. 2008.

[2] J. Mairal, M. Elad, and G. Sapiro, "Sparse representation for color image restoration," *IEEE Trans. Image Process.*, vol. 17, no. 1, pp. 53–69, Jan. 2007.

[3] M. Lustig, D. Donoho, and J. M. Pauly, "Sparse MRI: The application of compressed sensing for rapid MR imaging," *Magn. Reson. Med.*, vol. 58, no. 6, pp. 1182–1195, 2007.

[4] S.-I. Lee, H. Lee, P. Abbeel, and A. Y. Ng, "Efficient ℓ_1 regularized logistic regression," in *Proc. Assoc. Adv. Artif. Intell.*, 2006, pp. 401–408.

[5] E. J. Candes and T. Tao, "Decoding by linear programming," *IEEE Trans. Inf. Theory*, vol. 51, no. 12, pp. 4203–4215, Dec. 2005.

[6] E. Candes, T. Tao *et al.*, "The Dantzig selector: Statistical estimation when p is much larger than n," *Ann. Statist.*, vol. 35, no. 6, pp. 2313–2351, 2007.

[7] S. Becker, J. Bobin, and E. J. Candès, "NESTA: A fast and accurate first-order method for sparse recovery," *SIAM J. Imag. Sci.*, vol. 4, no. 1, pp. 1–39, 2011.

[8] W. Yin, S. Osher, D. Goldfarb, and J. Darbon, "Bregman iterative algorithms for l1-minimization with applications to compressed sensing," *SIAM J Imag. Sci.*, vol. 1, pp. 143–168, 2008.

[9] I. Daubechies, M. Defrise, and C. De Mol, "An iterative thresholding algorithm for linear inverse problems with a sparsity constraint," *Commun. Pure Appl. Math.*, vol. 57, no. 11, pp. 1413–1457, 2004.

[10] T. Blumensath and M. E. Davies, "Iterative thresholding for sparse approximations," *J. Fourier Anal. Appl.*, vol. 14, nos. 5/6, pp. 629–654, 2008.

[11] U. S. Kamilov and H. Mansour, "Learning optimal nonlinearities for iterative thresholding algorithms," *IEEE Signal Process. Lett.*, vol. 23, no. 5, pp. 747–751, May 2016.

[12] C. J. Rozell, D. H. Johnson, R. G. Baraniuk, and B. A. Olshausen, "Sparse coding via thresholding and local competition in neural circuits," *Neural Comput.*, vol. 20, no. 10, pp. 2526–2563, 2008.

[13] L. Yu, G. Zheng, and J.-P. Barbot, "Dynamical sparse recovery with finite-time convergence," *IEEE Trans. Signal Process.*, vol. 65, no. 23, pp. 6146–6157, Dec. 2017.

[14] Z. Yan, X. Le, S. Wen, and J. Lu, "A continuous-time recurrent neural network for sparse signal reconstruction via ℓ_1 minimization," in *Proc. Eighth Int. Conf. Inf. Sci. Technol.*, 2018, pp. 43–49.

[15] L. Zhu, J. Wang, X. He, and Y. Zhao, "An inertial projection neural network for sparse signal reconstruction via ℓ_{1-2} minimization," *Neurocomputing*, vol. 315, pp. 89–95, 2018.

[16] A. Wibisono, A. C. Wilson, and M. I. Jordan, "A variational perspective on accelerated methods in optimization," *Proc. Nat. Acad. Sci.*, vol. 113, no. 47, pp. E7351–E7358, 2016.

[17] A. Polyakov, D. Efimov, and B. Brogliato, "Consistent discretization of finite-time and fixed-time stable systems," *SIAM J. Control Optim.*, vol. 57, no. 1, pp. 78–103, 2019.

[18] A. Balavoine, C. J. Rozell, and J. Romberg, "Convergence speed of a dynamical system for sparse recovery," *IEEE Trans. Signal Process.*, vol. 61, no. 17, pp. 4259–4269, Sep. 2013.

[19] S. Shapero, C. Rozell, and P. Hasler, "Configurable hardware integrate and fire neurons for sparse approximation," *Neural Netw.*, vol. 45, pp. 134–143, 2013.

[20] S. P. Bhat and D. S. Bernstein, "Finite-time stability of continuous autonomous systems," *SIAM J. Control Optim.*, vol. 38, no. 3, pp. 751–766, 2000.

[21] A. Polyakov, "Nonlinear feedback design for fixed-time stabilization of linear control systems," *IEEE Trans. Autom. Control*, vol. 57, no. 8, pp. 2106–2110, Aug. 2012.

[22] I. Ekeland and R. Temam, *Convex Analysis and Variational Problems*. Philadelphia, PA, USA: SIAM, 1999.

[23] K. Garg, M. Baranwal, R. Gupta, and D. Panagou, "Fixed-time stable proximal dynamical system for solving mixed variational inequality problems," 2019, *arXiv:1908.03517*.

[24] S. Hassan-Moghaddam and M. R. Jovanović, "On the exponential convergence rate of proximal gradient flow algorithms," in *Proc. 57th Conf. Decis. Control*, 2018, pp. 4246–4251.

[25] H. H. Bauschke and P. L. Combettes, *Convex Analysis and Monotone Operator Theory in Hilbert Spaces*. New York, NY, USA: Springer, 2017.

[26] A. Balavoine, C. J. Rozell, and J. Romberg, "Discrete and continuous-time soft-thresholding for dynamic signal recovery," *IEEE Trans. Signal Process.*, vol. 63, no. 12, pp. 3165–3176, Jun. 2015.